OWL opto-mechanics, phase A.

E. Brunetto, M. Dimmler, F.Koch, M Quattri (European Southern Observatory).
M.Müller (TU Munich). B.Sedghi (EPF Lausanne).

ABSTRACT

The "phase A" of the opto-mechanical design, which started in 1997, is now basically completed. It provides a clean, symmetrical geometry of the pupil, with a near-circular outer edge. The modular design of the mechanical structure is built on the size of the hexagonal segments, provides a perfect match with the optical elements and allows production at reasonable costs. This paper is a summary of the various design iterations. A discussion is devoted to the evaluation of the design assumptions and principles which have been set at the beginning of the study, and to their validity after the completion of this first phase. This includes a discussion about specific aspects whose criticality had been under- or overestimated, and the methodology applied to define system and sub-system requirements. Finally, we present a summary of the present and future activities, which are mainly devoted to sub-systems definition.

Keywords: Telescope, structure, opto-mechanics, analysis, control.

1. INTRODUCTION

The design principles and assumptions, set at the very beginning of OWL design [1], have been followed during the numerous design iterations which took place since 1997. Constant monitoring of the costs and special attention to safety aspects have accompany and shaped the design process.

DESIGN PRINCIPLES.

- Maximize dynamic and static performance.
  - ⇨ Minimize mass.
  - ⇨ Embedded configuration (low Center of Gravity).
- Manufacturing.
  - ⇨ Existing technology, availability.
  - ⇨ Mass produced modular system.
- Assembly, Integration and Verification.
  - ⇨ Transport (maximum size).
  - ⇨ Assembly (Self standing).
  - ⇨ Instrument.
  - ⇨ Metrology.
- Operations.
  - ⇨ Low thermal inertia.
  - ⇨ Wind disturbance.
- Maintenance.
  - ⇨ Segment re-coating
  - ⇨ Access to sub-systems

DESIGN ASSUMPTIONS.

Soil characteristic, value range:
- ⇨ Paranal 50000 MPa.
- ⇨ La Palma 5000 MPa.

Existing infrastructures within reasonable distance.
- ⇨ Harbor.
- ⇨ Roads.

Seismicity 0,2 g, intermediate value between:
- ⇨ Paranal 0,34 g
- ⇨ La Palma 0,06 g.

Wind, observation mode.
- ⇨ 10 m/s.

2. DESIGN EVOLUTION

The performance and cost of the project have been monitored by essentially analyzing the locked rotor frequency and the total rotating mass of the telescope. These two values give a rough evaluation of how good the telescope will perform and how much it will cost. The two diagrams below summarize the trend of these two key parameters during the design evolution. It has to be underlined that the degree of accuracy and details of the telescope design, has increased constantly, in accordance to the information which became available from engineering studies of sub-systems, industrial verification studies and the evolution of the optical design. The latest design iteration also includes a 500 tons, allocation which takes into account auxiliary equipments like: staircases, lifts, floors, cat walks, cabling, electronic

cabinets and piping, on board maintenance and handling, localized air conditioning, thermal insulation, cable wraps and paint (50 tons).

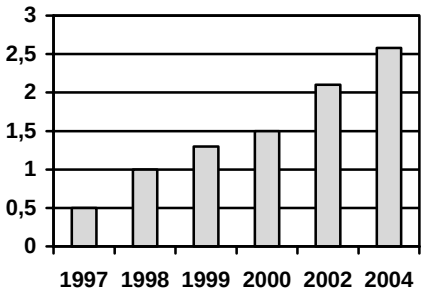

Figure 2: Locked rotor frequency evolution [Hz]

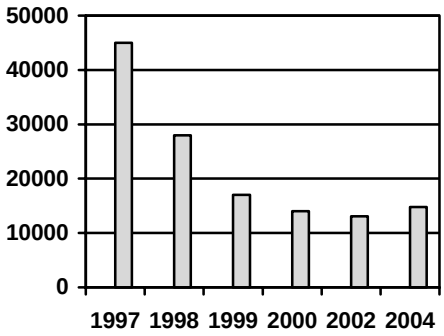

Figure 1: Mass evolutions [tons].

3. DESIGN STATUS

The telescope design is based on existing technologies and materials.

- Telescope trusses structure made of mild steel.
- Mirror substrate made of glass ceramic.

OWL's dimensions allow to rely extensively on modular design, integration and maintenance, with large numbers of identical parts, components and modules. As a result, construction and operation costs are very low for a system of this size and capability, and multiple supply and integration lines allow a fast construction schedule. Virtually all telescope parts can be shipped to the site in standard 20 or 40ft containers. The alt-az structure of the telescope is embedded into the foundation, thus minimizing the detrimental soil impact on the performance; the drive are located far from the center of rotation and on-board facilities are reduced to the minimum.

Telescope major Characteristics:

- Six fold symmetry.
- Six focal stations.
- Improved diffraction pattern.
- Near-circular M1.
- Matching symmetries of the structure and segments.
- Up to 60º observation mode.
- Up to ±90º maintenance mode.
- Latest iteration: segment size 1.6-m
  - M1 3048 segments.
  - M2 216 segments.

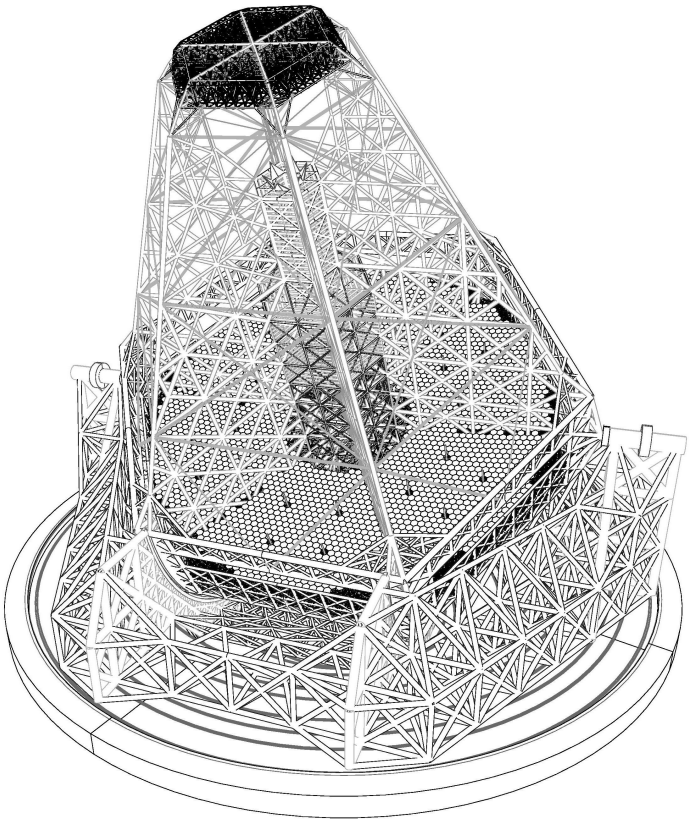

Figure 3: Telescope layout.

3.1. Structure design.

The trusses structure of the telescope is based on an aptly named "Fractal Design", which is basically a repetition of modules scaled from the triangular six fold symmetry of the mirror segments. The basic prism pattern is shown in Figure 4. This fractal design makes not only the mass production of the steel structure possible, but also assures an even transfer of loads and forces from the optical elements to the telescope foundation. The possibility of implementing inner air ventilation of the structure, envisaged at the very beginning of the design, is still valid and it can be implemented if environmental condition would require it.

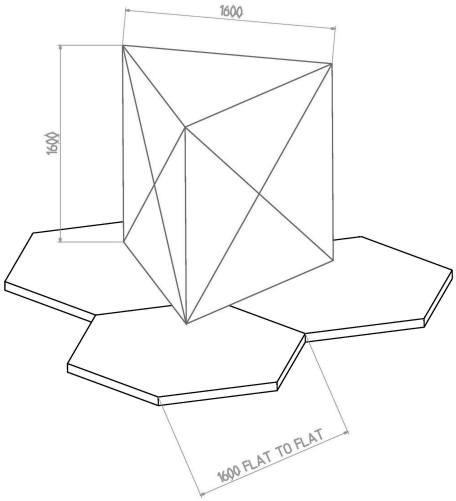

Figure 4: Fundamental parallel prism pattern.

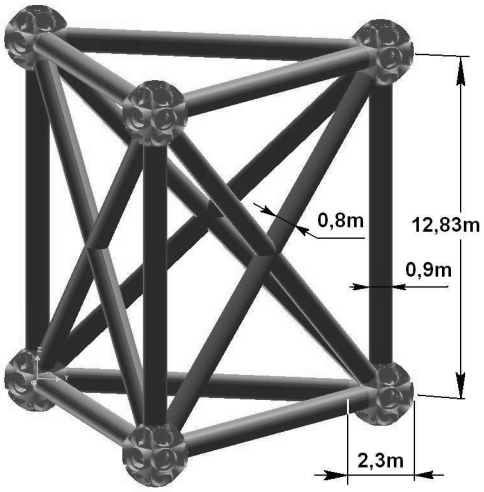

Figure 5: Structure module.

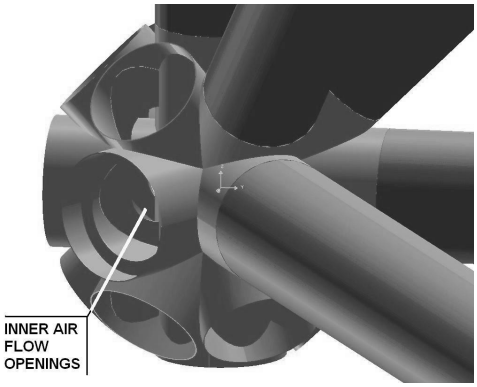

Figure 6: Node assembly

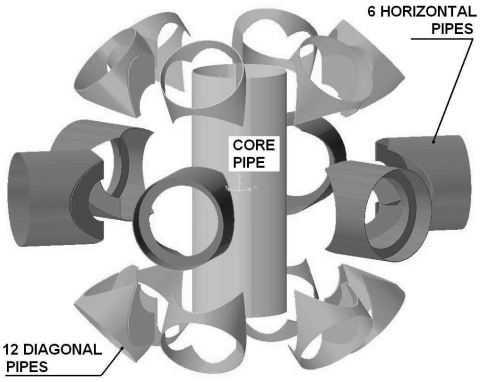

Figure 8: Node weld assembly.

In order to maximize the benefits of mass production elements, each node can be assembled using only three types of parts (see **Figure 8**) and transported in standard containers. The feasibility of the nodes mass production and its related costs and schedule, have been validated by an industrial study.

Figure 7: Transport of nodes.

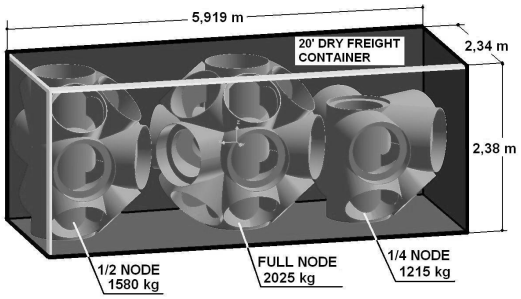

3.2. Sub-systems design.

In this section only the main telescope opto-mechanical sub-systems which have a critical impact in term of performance, schedule and costs are discussed.

3.2.1. Kinematics.

The main axes kinematics relay on Friction Drive and Bearing, which has already been extensively discussed and reported [2]. The assumptions and trade-offs which led to this concept are still applicable to the present OWL's design. All the Bogies (246 azimuth and 154 altitude) have been modeled , in term of stiffness and mass and implemented into the OWL FEM, as described in section 4. The problems related to the main axes control under friction and wind disturbances are reported in section 4.

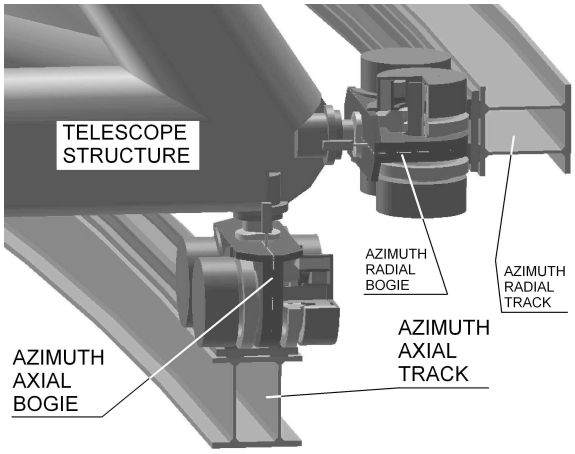

Magnetic Levitation (MagLev), which is under development for several transportation projects, could be an interesting alternative to Friction Drive and Bearing. A first evaluation run shows that the main potential advantages of friction less, high tunable stiffness, low mechanical tolerances (tracks) and virtually maintenance free operation have to be traded-off with energy consumption and realization costs. It is planned to perform a feasibility study on this technology applied to telescope requirements.

Figure 9: Friction Drive and Bearing.

3.2.2. Segments support system.

The large amount of segments (>3000) which have to be kept phased under gravity, thermal and wind disturbances, and the associated costs, make of the segments support system one of the most critical part of the telescope. The design is in a conceptual phase and it has to be validated by industrial study, demonstrators and tests.

Segment Support System requirements:

- Three Position Actuators
  - Fine Actuator Stage. Accuracy ± 5 nm. Stroke 0,5 mm.
  - Coarse Actuator Stage. Accuracy ± 0.05 mm. Stroke 20 mm.
- Extractor. Stroke 160 mm
- Axial resonance frequency > 60 Hz.
- Edges Sensors. Resolution 0,5 nm. Shear stroke 0,5mm. Reading 20 Hz.

This configuration concept allows:

- Ample design volume.
- Large mass budget.
- Electronics located in the very vicinity of the Position Actuators.
- Easy access.
- Comfortable integration and maintenance operations.
- Safe operations.
- Low mechanical "cross talk" betweenbetween Position Actuators.
- Excellent load transfer to the mirror cell mechanical structure.
- Simple and stiff whiffle tree design.

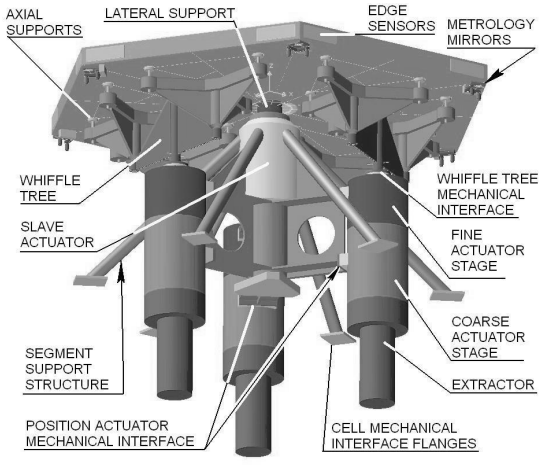

Figure 10: Segment Support System

All the Segment Support Systems and their segments have been modeled and implemented into the OWL FEM, described in section 4.

3.2.3. Corrector

The corrector contains the active and adaptive large optical elements of the telescope. It provides re-center, re-focus and correction for large displacements and tilts due to gravity and thermal disturbances. Its optical elements and characteristics are described in [3]. Due to the high stiffness of the telescope structure the stroke of the actuators is limited to few mm with an accuracy of about 0,1 mm. The total moving mass of the corrector is about 130 tons, similar to the VLT tube system. The ample design space and its location in one of the stiffest parts of the telescope facilitate the design of the corrector. Inside the corrector, the most critical part remains the M6, which is adaptive and provides fast field stabilization around 2 axes. The telescope structure surrounding the corrector is thermally insulated and air conditioning is provided only within the inner volume occupied by the corrector. A set of flaps ensures natural ventilation, as in the VLT enclosure, during observation. The corrector can be integrated in to the telescope structure via a central corridor, with the altitude structure in horizontal parking position.
All the optical elements and their support actuators, have been modeled as lump masses and implemented into the OWL FEM, described in section 4. The actuator axial stiffness has also been modeled.

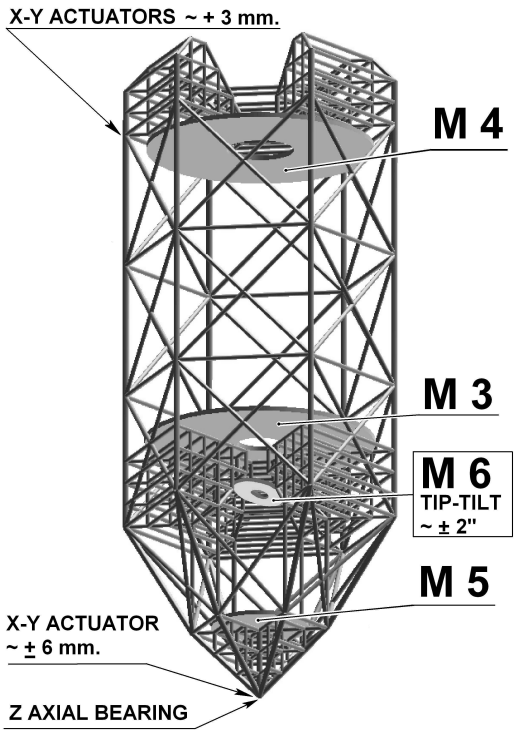

Figure 11: Corrector assembly.

3.2.4. Instrumentation rooms

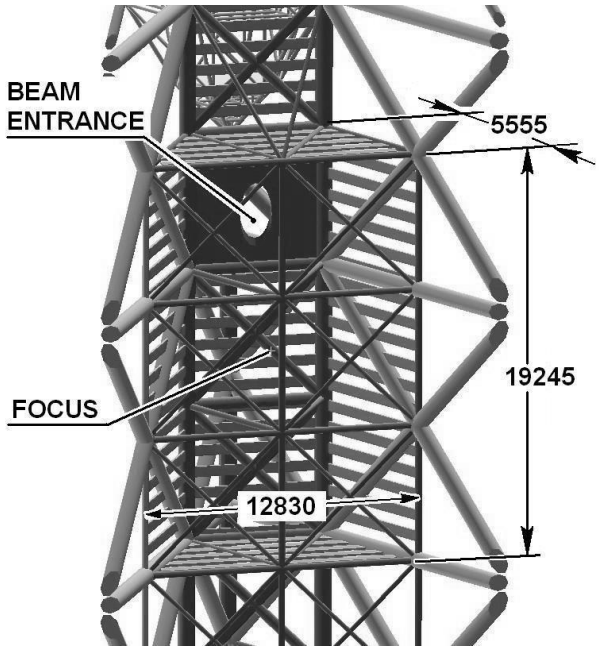

The six fold symmetry of the telescope structure, allows to accommodate 6 instrumentation rooms, arranged symmetrically around the telescope altitude structure centre axis. The optical beam can be sent to any of these 6 focal stations by simple rotation of M6. Each instrument can have a mass of up to 15 tons which have been modeled as lump masses and implemented into the OWL FEM, described in section 4. The shape of each room is a prism with a trapezoidal base (see). The ample design space and its location in one of the stiffest part of the telescope facilitate the design of the instruments. Several structural nodes serve as mechanical interfaces to the instruments. The telescope structure surrounding the instrumentation rooms is thermal insulated and air conditioning is provided only to the room inner volume. A set of flaps ensures natural ventilation, similar to the VLT enclosure, during observation. Easy access to the rooms is provided by lifts and stairs.

Figure 12: Instrumentation room

3.2.5. Mass breakdown.

The total rotating mass of the telescope is a remarkably low for a rotating structure of the OWL's size. In order to better appreciate this result, it can be illustrative to "collapse" the structural steel and glass ceramic materials in cubes, then evaluate the aspect ratio between the size of the telescope and the size of the cubes. Doing the same exercise with the VLT telescope, one can realize the improvement. A VLT scaled up to a 100 m aperture would have a structural steel material mass of 679876 tons, with catastrophic impact on stresses.

SUB-SYSTEMS.	Corrector [Tons]	Altitude structure [Tons].	Total Mass. [tons].
M1 - 3048 glass ceramic hexagonal segments.		1158,2	
M1 whiffle tree and actuators.		304,8	
M2 - 216 glass ceramic hexagonal segments.		82,08	
M2 whiffle tree and actuators.		21,6	
M3 and actuators.	31,5		
M4 and actuators.	30,5		
M5 and supports.	8,25		
M6, tip-tilt cell and actuators.	2,07		
Corrector steel pipes structure.	57		
Total corrector unit.	**129,32**	129,32	
Instrumentations (6 instruments).		90	
Altitude structure steel pipes and kevlar ropes.		7242	
Total altitude structure.		**8916,7**	8916,7
Total azimuth structure.			5415,9
Miscellaneous (electronics, cabling, piping, stairs, lifts, cat-walks, paint, welds etc.)			500
Total telescope rotating mass.			**14832,6**
Azimuth tracks.			~ 4500

Table 1: Mass breakdown.

Figure 13: OWL structural material.

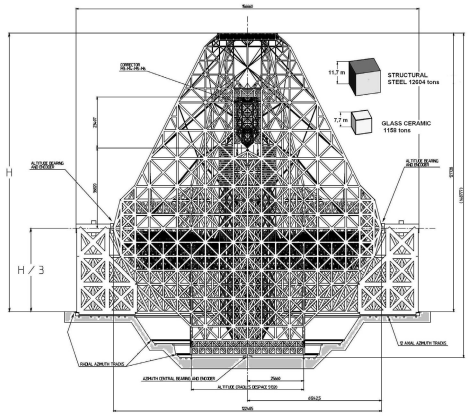

IF VLT WERE BASED ON OWL DESIGN.
M1 thickness 6 mm.
Steel mass 7,5 tons.

↔

IF OWL WERE BASED ON VLT DESIGN.
Steel mass 679876 tons.
M1 thickness 2 m.

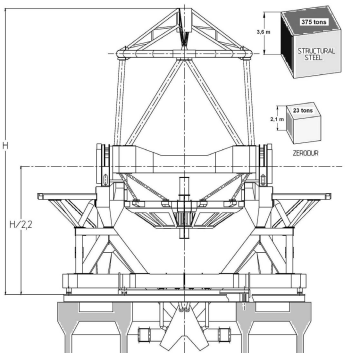

Figure 14: VLT structural material.

3.3. Enclosure.

Figure 15: Enclosure lay-out.

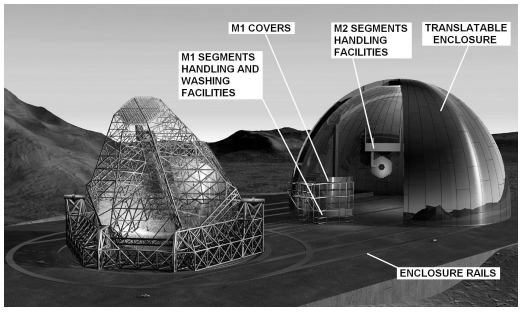

OWL is designed to be operated in open air. A sliding enclosure protects the telescope during day time and in case of adverse weather condition. The inner enclosure volume allows full rotation of the telescope alt-az axes. The enclosure concept is based on existing projects. The enclosure feasibility, costs and schedule are for the time being evaluated. A feasibility study is planed to quantify cost and schedule according to OWL requirements on two representative sites. Other function like M2 segment handling can be integrated in the enclosure. The M1 covers and M1 segment handling and washing unit, remain external to the telescope and can be translated independently from the enclosure, thus reducing the shut down time.

4. ANALYSES

4.1. FE Model and Assumptions

The FE Model of OWL is displayed in Figure 16. It comprises the rotating parts of the Altitude and Azimuth structures and consists of about 146000 elements. The steel framework structure is modelled with pipe elements and the ropes with link elements. The primary mirror segments as well as the mirrors M3 to M6 are represented as distributed mass elements, which are linked to the cell structures by appropriate beam elements. The secondary mirror segments are modelled as rigid shell elements, which are connected to the M2 cell structure by appropriate beams simulating the stiffness and weight of the segment support structure (see detail in Figure 17). All the mirror masses are based on Zerodur material.

All the bogies are modelled as simple beam elements to simulate their stiffness and mass. The contact stiffness between the bogies' wheels and the rails has been taken into account. Fixed boundary conditions are applied to the Azimuth bogies at the interface to the rails.

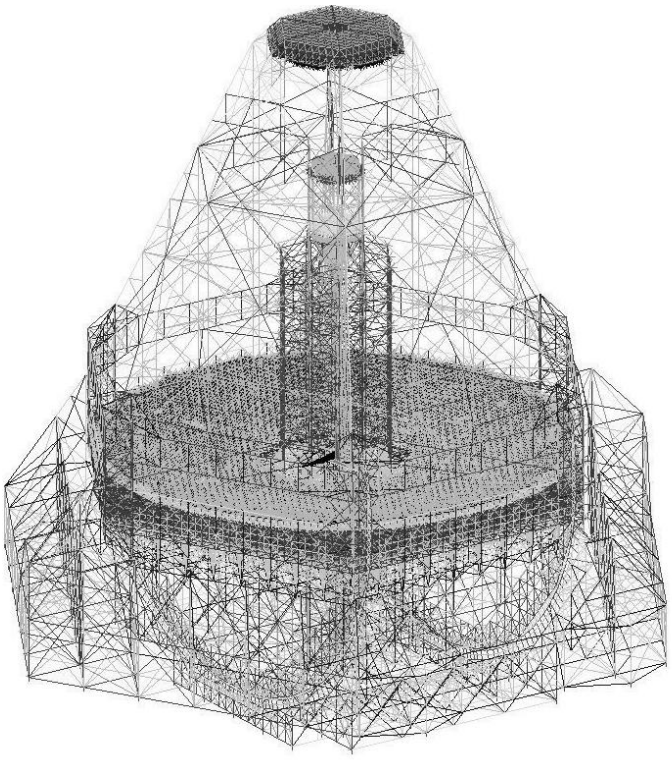

Figure 16: FE Model of OWL "phase A" design.

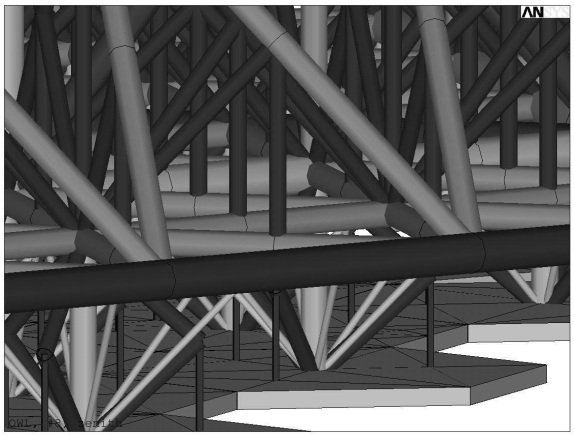

Figure 17: FE Model detail of M2 segment support.

The total mass of the FE Model corresponds to the mass breakdown (Table 1). In order to take into account the "miscellaneous" additional mass allocation of 500 tons, the density of the steel has been adapted accordingly. The Kevlar ropes are represented as link elements which transmit only longitudinal forces.

Three FE models with different altitude configurations have been investigated (zenith, 30º and 60º from zenith). For the non-zenith configurations the number of contacting "altitude" bogies is reduced.

4.2. Modal Analyses

Modal analyses of the three Altitude configurations have been carried out. Table 2 to Table 3 summarise the predominant eigenfrequencies of all three configurations as well as their effective masses and mode shapes.

Mode	Frequency	Effective mass / inertia in % of total						Mode shape
		MX	MY	MZ	IXX	IYY	IZZ	
1	1.59	67	-	-	-	2	-	Cross elevation
2	**2.58**	**-**	**30**	**-**	**29**	**-**	**-**	**Altitude locked rotor**
3	2.86	-	-	-	-	-	44	Azimuth locked rotor
6	3.67	-	35	-	12	-	-	2nd alt. locked rotor (counter motion)
7	**3.93**	**-**	**-**	**11**	**-**	**-**	**-**	**Piston M2**
8	4.03	-	-	46	-	-	-	Piston altitude structure

Table 2: Eigenfrequencies and effective masses of zenith configuration.

Mode	Frequency	Effective mass / inertia in % of total						Mode shape
		MX	MY	MZ	IXX	IYY	IZZ	
1	1.55	67	-	-	-	2	-	Cross elevation
2	**2.49**	**-**	**27**	**-**	**31**	**-**	**-**	**Altitude locked rotor**
3	2.92	-	-	-	-	-	42	Azimuth locked rotor
6	3.83	-	30	3	10	-	-	2nd alt. locked rotor (counter motion)
7	**3.92**	**-**	**-**	**47**	**-**	**-**	**-**	**Piston Altitude structure**

Table 3: Eigenfrequencies and effective masses of 30 º configuration.

Mode	Frequency	Effective mass / inertia in % of total						Mode shape
		MX	MY	MZ	IXX	IYY	IZZ	
1	1.56	67	-	-	-	2	-	Cross elevation
2	**2.06**	-	28	1	32	-	-	**Altitude locked rotor**
3	2.83	-	-	-	-	1	39	Azimuth locked rotor
6	**3.63**	**-**	**18**	**28**	**28**	**-**	**-**	**Piston and Altitude bending**
7	3.78	-	14	22	22	-	-	2nd piston and alt. rotor (counter m.)

Table 4: Eigenfrequencies and effective masses of 60 º configuration.

The lowest natural frequency for all configurations is the cross elevation mode at about 1.6 Hz, which is a lateral motion of the Altitude structure along the altitude axis. The most important modes in terms of axis controllability are the locked rotor frequencies about the altitude and azimuth axis, respectively. While the Azimuth locked rotor frequency is similar for all configurations, the Altitude locked rotor frequency decreases from 2.58 Hz at zenith down to 2.06 Hz at 60º from zenith. This performance reduction is caused by the reduced number of altitude bogies in contact. The lowest piston mode of the M2 structure is calculated to be 3.93 Hz for zenith and 3.63 Hz for 60º from zenith. A typical altitude locked rotor mode shape in zenith configuration at 2.58 Hz is shown in Figure 18. As already mentioned earlier a significant improvement of the dynamic performance in terms of locked rotor eigenfrequencies has been obtained, i.e. more than 20 % frequency increase compared to the former design iteration (2002).

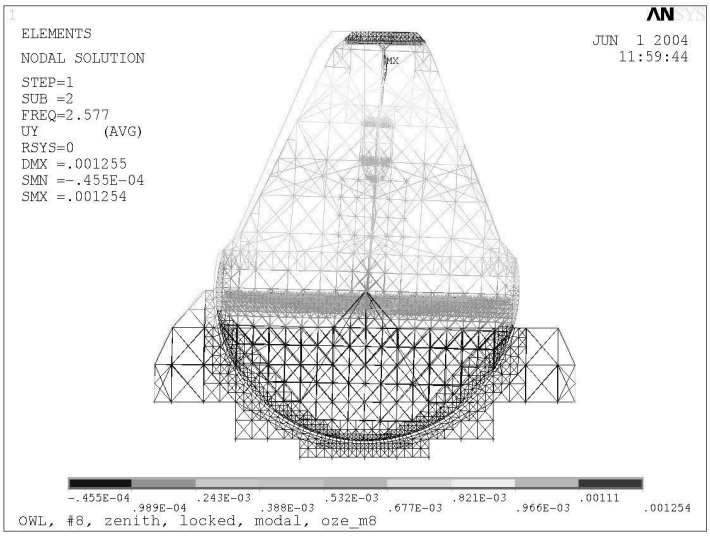

Figure 18: Locked Rotor mode shape in zenith configuration at 2.58 Hz.

4.3. Static Analyses

In order to predict the required range of the various position actuators of the mirror segments and the corrector structure, the displacements of the primary and secondary mirrors have been calculated under gravity load and steady state wind loading. Again different altitude axis configurations have been investigated to evaluate the maximum mirror motions within the operational range.

4.3.1. Gravity

The rigid body (r.b.) displacements listed in Table 5 correspond to the global best-fit deformations of the primary and secondary mirror segments in terms of piston, tilt and decenter. These displacements are the differential values when moving the telescope from zenith down to 60 º from zenith. As it is foreseen to correct these errors by the corrector actuators, only the differential piston and tilt between M1 and M2 has to be considered. The error caused by the decenter depends only from the primary decenter, because the secondary mirror is flat. Therefore, to compensate for gravity effects, the minimum required corrector actuator strokes are 3.4 mm (piston), 2.1 arcsec (tilt) and 13.2 mm (decenter).

In order to define the required strokes of the segment position actuators, the PTV displacements of the primary and secondary mirror segments have been evaluated and the worst case values summarised in Table 5. Hence, the total required coarse segment actuator stroke results in **11 mm**, which includes 10.1 mm from the M1 piston and 0.9 mm from the mirror segments tilt, i.e. 147 arcsec tilt correspond to 0.9 mm actuator piston assuming an actuator distance of 1.2 m. In order to be conservative, the worst case displacements of M1 and M2 have been selected to evaluate the required stroke range.

Mirror	Piston [mm]		Tilt [arcsec]		Decenter [mm] [1]	
	r.b.	PTV	r.b.	PTV	r.b.	PTV
M1	-7.8	**10.1**	0.1	**147**	**-13.2**	**8.8**
M2	-11.2	2.8	-2.0	133	-30.8	1.1
M2 – M1 [2]	**-3.4**		**-2.1**		-17.6	

Table 5: Rigid body displacements under 60 º altitude axis rotation

4.3.2. Wind load

To estimate the steady state contributions from wind loading, the displacements of M1 and M2 have been calculated for a mean wind speed of 10 m/s. The applied wind forces correspond to a wind speed profile ranging from zero (ground surface level) up to 13.2 m/s (M2 level) and are based on conservative drag coefficient assumptions. Table 6 provides a summary of the rigid body and PTV displacements, respectively. The displacements are worst case values out of three different altitude configurations (zenith, 30 º and 60 º from zenith).

As can be seen from the rigid body results, the worst piston (0.41 mm) and tilt (1.3 arcsec) values are obtained for the 60 º configuration. The PTV deformations caused by steady state wind are below 0.6 mm for piston and 6.5 arcsec for tilt. Due to the small best-fit deformations, one could consider compensating these errors together by the fine segment position actuators.

Mirror	Piston [mm]		Tilt [arcsec]		Decenter [mm]	
	r.b.	PTV	r.b.	PTV	r.b.	PTV
M1	-0.29	**0.60**	**1.30**	4.57	**-0.18**	**0.11**
M2	**-0.41**	0.16	1.21	**6.32**	-0.80	0.03
Worst case configuration	60 º	60 º	60 º	30 º	30 º	30 º

Table 6: Rigid body displacements under steady state wind load.

[1] The decenter of M2 is provided for information only, because it has no impact on the image motion due to its flat surface.

[2] To be corrected by Corrector actuators.

4.4. Main axes control.

The Kinematics concept is based on bogies [2], with about 250 friction drives (bogies) for the azimuth axis and 150 bogies for the altitude axis. The large amount of bogies ensures a homogenous load transfer to the foundation. As shown in Figure 9 each friction drive consists of four spherical or cylindrical wheels, which are independently driven by brushless ring torque motors. The bogies roll on tracks and the wheel/track friction plays an important role for the behavior of the system. A control study has been performed addressing a strategy for friction compensation and coordination of groups of bogies. The main goal was to minimize the residual tracking errors due to friction, i.e. stick-slip effects.
As a preparation for the main study, ANSYS finite element models were translated into reduced order MATLAB models using the Structural Modeling Interface (SMI) toolbox (see Figure 19).

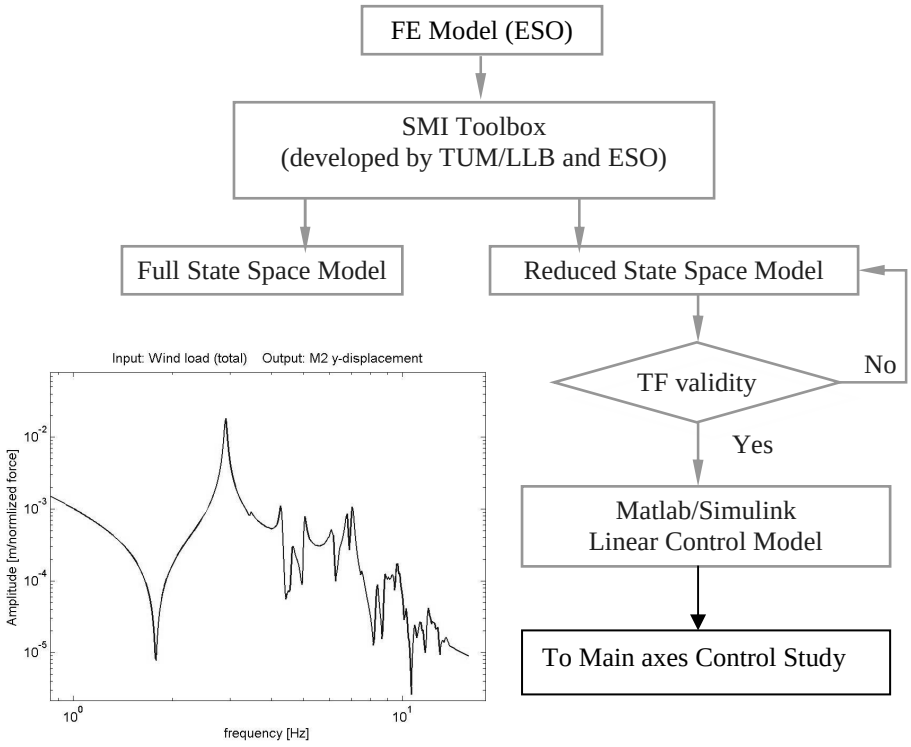

Figure 19: Converting FE Models into State-Space Models SMI

The main study, shown in Figure 20, was split into 4 steps, from which the first 3 are completed by the time of writing this article.

1. Linear Case Study: A control strategy and achievable performances were given for the case where the telescope is supposed to be driven by an ideal torque generator. The aim of this step was to define the possible targets for an ideally working friction compensation scheme. The main disturbances were wind loads at different locations provided as PSDs and time series. The design goal was to minimize the residual tracking error for different wind load cases and telescope orientations. The controller design is based on a loop-shaping method using high order polynomial controllers.

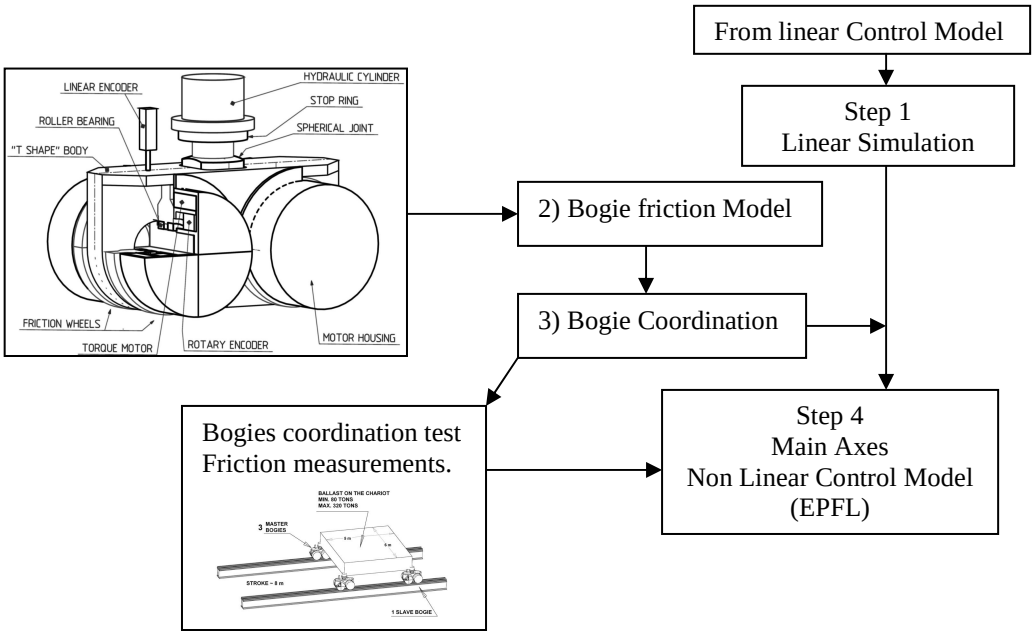

Figure 20 OWL Main Axes Control Study

2. Bogie Friction Drive System: Two suitable friction models for the simulation of the friction drive system were proposed, the Karnopp and the LuGre model [3]. For the study of this step the telescope was supposed to be rigid. The simulation results showed that both friction models, except in the pre-sliding regime, give similar results. In particular, the stick-slip behavior could be predicted with both models. An important detail of the study was the distinction of two types of friction acting on the bogies: rolling and sliding friction (see Figure 21). The rolling friction contribution (due to deformation of surface and distribution of the normal force over the actual contact area) causes the main difficulties for the control of the axes whereas the sliding friction is necessary to avoid the sliding of the bogies on the tracks.

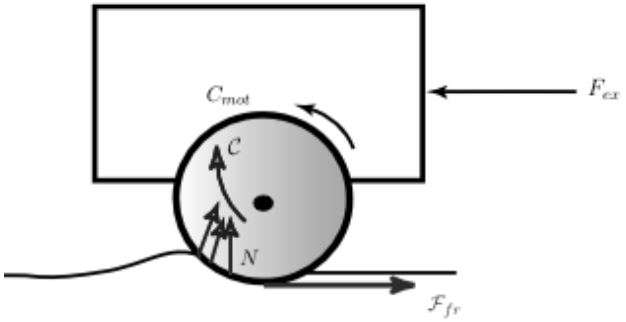

Figure 21 Rolling and Sliding Friction of a Bogie: Rolling friction C – Sliding friction F_{fr}

3. Coordination of Bogies: A model was given coordinating several active (driven) and passive (non-driven) bogies. As in step 2 the telescope was supposed to be rigid. In this model a control strategy using a feed-forward friction compensation was applied. It was shown that for a position ramp reference signal the non-linear effect of friction could be eliminated (see Figure 22). The issue of parameter mismatch (variation) for the estimated friction parameters was investigated and guidelines for experiments and friction parameter estimations were derived. The telescope position error calculated for OWL's smallest ~ Ø 50 m track, and measured at center azimuth axis encoder location are: 2.1 arcsec without compensation and 0.17 arcsec with compensation.

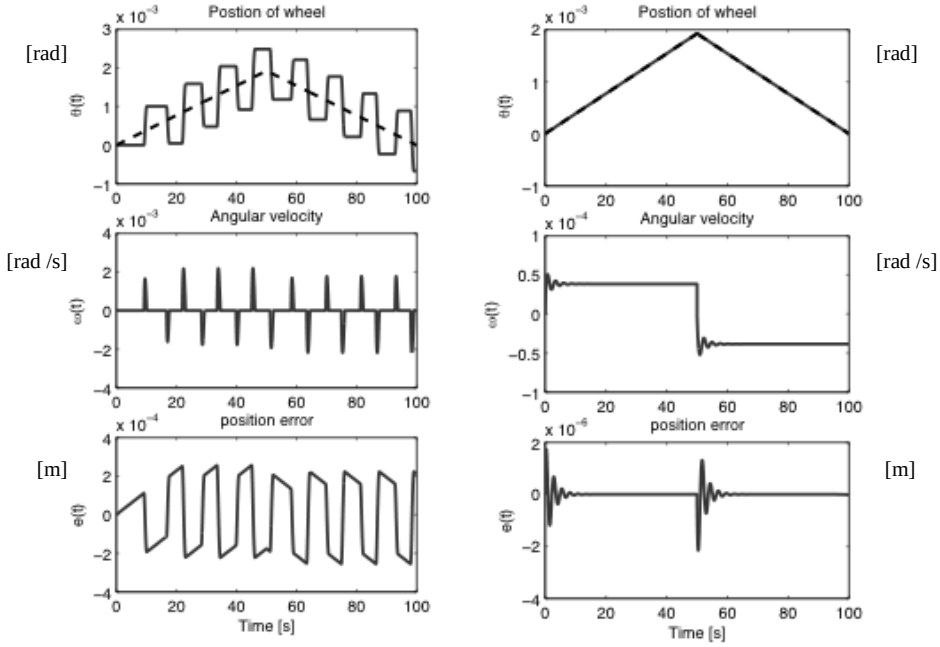

Figure 22 Avoiding Stick-slip Motion by Feed-Forward Friction Compensation:
Bogie system response without compensation (left) – response with compensation (right)

4. Complete system: This last step of the main axes control study will try to bring the results of the former steps together and combine the linear controller approach with the proposed feed-forward friction compensation scheme. The complete results are expected by end of August 2004.

5. CONCLUSIONS.

The latest results obtain at the end of phase A show a very robust and lightweight telescope structure, thereby providing a reliable baseline for low level requirement definition of the various telescope sub-systems. Several studies, sub-systems design, demonstrators, prototypes and tests are running or planned for the next 3 years. The most critical are: control simulations (Main axes, corrector, field stabilization, segments phasing.), wind measurement and analysis [4], diffraction effects study, segments support system design, segments phasing under wind disturbance, foundation model, enclosure conceptual design, maintenance equipment, handling equipments, internal metrology and many other. Meanwhile essential information, like site (wind and soils model), instrumentation design and AO, segments substrate and optical design update, will be available for the final opto-mechanical optimization of the project. Although wind disturbance on OWL's large optical surfaces has always been recognized as one of the most critical part of the project, the wind characterization turns out to be unexpectedly difficult to define. Computational Fluid Dynamic can not resolve at segment to segment scale at high temporal frequencies and wind tunnel measurement need an independent validation. Therefore a wind pressure measurement campaign has been initiated on a 76 m radio telescope [4]. The Lowell telescope at JBO has been chosen because of its configuration and site characteristic, which match OWL's wind characterization requirements.

6. REFERENCES.

1. OWL: First steps towards designing the mechanical structure. Bäckaskog Workshop on ELT 1999.
2. Friction drive and bearing for OWL's main axes, technological step backwards or cost effective alternative? SPIE Future Giant Telescope 2002. [4840-33].
3. F.Altpeter, "Friction Modeling, Identification and Compensation", Ph.D. Thesis, EPF Lausanne (1999).
4. Pressure measurements on the 76-metre Jodrell Bank radio telescope and a scaled down model in the wind tunnel. At this conference [5497-74].